Development of a Streak-Camera-Based Time-Resolved Microscope Fluorimeter and Its Application to Studies of Membrane Fusion in Single Cells[†]

Akihiro Kusumi,*,‡,§ Akihiko Tsuji,‖ Masayuki Murata,⊥ Yasushi Sako,‡ Akiyasu C. Yoshizawa,⊥ Satoshi Kagiwada,⊥ Tsuyoshi Hayakawa,‖ and Shun-ichi Ohnishi⊥

Department of Pure and Applied Sciences, College of Arts and Sciences, The University of Tokyo, Meguro-ku, Tokyo 153, Japan, National Biomedical ESR Center, Department of Radiology, The Medical College of Wisconsin, Milwaukee, Wisconsin 53226, Central Research Laboratory, Hamamatsu Photonics K. K., Hamakita 434, Japan, and Department of Biophysics, Faculty of Science, Kyoto University, Kyoto 606, Japan

Received November 27, 1990; Revised Manuscript Received April 2, 1991

ABSTRACT: A time-resolved microscope fluorimeter based on a synchroscan streak camera and a fast pulsed laser system has been developed to measure the fluorescence lifetime decay under the fluorescence microscope. This system allows one to measure the nanosecond fluorescence lifetimes of fluorophores in a small spot (0.8–6.3 μm diameter) in single cultured cells under a fluorescence microscope, while the cells are being viewed under a high-power objective lens. A signal acquisition time between a second and a minute was usually sufficient to obtain fluorescence decay curves with good quality for 10^3–10^5 fluorophores localized in 1 μm^2 domain. A signal-to-noise ratio better than 30 was obtained for $\approx$30 000 fluorescein-labeled band 3 molecules in a 2 μm^2 region in a single human erythrocyte ghost after signal accumulation for 30 s. The measured lifetimes for a variety of fluorescent probes attached to proteins in solution and lipids in liposomes showed a good agreement with those measured in a cuvette under standard conditions by time-correlated single photon counting. With the development of this instrument, microscope fluorimetry has become a practical, straightforward, quantitative technique for investigation of molecular processes in single cells in culture. Time-resolved microscope fluorimetry has been applied to observe fusion of liposomes in vitro and that of endosomes in single cells by monitoring resonance energy transfer. Inspection of individual liposomes and endosomes revealed the extent of fusion for each vesicle. Since the use of time-resolved microscope fluorimetry eliminates the need for subcellular fractionation or the complex correction procedures in steady-state microfluorimetry, it greatly simplifies the assay for endosome fusion in vivo. The results showed that extensive fusion of sequentially formed endosomes takes place all over the cell matrix in cultured cells. This suggests that extensive fusion with incoming endosomes takes place in many endosomal compartments, possibly sorting organelles, or that the early endosomes fuse with the preexisting network of tubular cisternae of the endosomal compartment at many points in the network. It is concluded that time-resolved microscope fluorimetry is a powerful noninvasive technique for studies of in situ biochemistry and biophysics using cells and tissues.

Fluorescence microscopy has been extensively utilized in biomedical research. The key point of the use of optical microscopy, including fluorescence microscopy, as compared to electron microscopy is that the former allows one to study *living* cells and tissues in culture. In addition, fluorescence microscopy provides high specificity and sensitivity. For example, immunofluorescence microscopy allows one to observe specific proteins that are present in 50 copies in a cubic micrometer volume (Taylor & Salmon, 1989).

The major drawback of fluorescence microscopy is its low spatial resolution (a few hundred nanometers), as compared to that of electron microscopy ($\approx$1 nm), which is determined by the diffraction limit of light and the finite numerical aperture of the objective lens. Due to the limitation of reso-

lution, fluorescence microscopy fails to provide information at the molecular level, such as intermolecular distances and molecular motion. As the result of the lack of molecular information in optical microscopy, it has always been difficult to correlate the biophysical and biochemical data obtained in vitro to the events occurring in living cells observed under an optical microscope. It would be highly desirable if one could gain molecular information in living cells while they are being viewed under the fluorescence microscope.

Spectroscopic measurement under the fluorescence microscope has been employed to obtain molecular information on the microscopic structure (Thaer & Sernetz, 1973). However, because of the difficulty in obtaining correct fluorescence spectra under the fluorescence microscope and in comparing two fluorescence spectra taken under different conditions (e.g., the sample and the control) due to the differences in the degree of light scattering, path length, and background fluorescence, fluorescence spectroscopy under the microscope has not become a prevalent technology. A more sound experimental observable that can be reliably measured under the fluorescence microscope was needed. In the present work, we have employed fluorescence lifetime decay as a spectroscopic observable and have undertaken to advance time-resolved microscope fluorimetry to perform nanosecond time-resolved

* Address correspondence to this author.
‡ The University of Tokyo.
§ The Medical College of Wisconsin.
‖ Hamamatsu Photonics K.K.
⊥ Kyoto University.

fluorescence measurements under the microscope. The excited-state lifetime would be the only physical observable, the absolute value of which could be precisely determined under the fluorescence microscope.

In a series of papers dating from the mid-70's, Sacchi and his collaborators (Sacchi et al., 1974; Andreoni et al., 1980; Docchio et al., 1982; Bottiroli et al., 1984) and Fernandez and his collaborators (Fernandez & Berlin, 1976; Herman & Fernandez, 1978, 1979, 1982; Fernandez, 1984) have pioneered time-resolved microscope fluorimetry. In addition, instrumentation for time-resolved fluorescence measurements under the microscope have been described by Alsins et al. (1982) and Minami and his collaborators (Minami & Hirayama, 1986; Minami et al., 1986; Wang et al., 1989). However, in spite of its potentially wide application, time-resolved microscope fluorimetry has not yet become popular mainly due to its technical difficulties: it is plagued by low sensitivity and, thereby, the long signal accumulation time. The long signal acquisition time required for obtaining an adequate signal-to-noise (S/N) ratio in the fluorescence lifetime decay curve has severely limited its use in biomedical studies, in which labile and/or ever-changing biological samples are used. The low sensitivity is inherent to this method because the fluorescence signal is collected from a region of a few square microns and time-resolved in the nanosecond time range.

In the present study, we have largely solved this problem by developing a synchroscan streak camera that operates at 4 MHz in synchrony with a pulsed laser system: since S/N can be improved by signal accumulation, and since we are dealing with labile biological samples, we concentrated our effort on performing the signal accumulation as fast as possible. With the developed instrument, the total fluorescence decays were collected at a rate of 4 MHz (487 points per decay), increasing the S/N of the decay curve by a factor of 2000 during the first second of data acquisition and by a factor of 16 000 during the first minute. The typical signal acquisition time is between 2 and 60 s.

The time-resolved microscope fluorimeter developed in this work has capabilities of temporal ($\approx$100 ps), spatial ($\approx$1 μm), and spectral ($\approx$10 nm) resolutions. It allows one to carry out in situ biochemistry and in situ biophysics to obtain molecular information in cells and tissues in culture.

We have applied this method to the studies of fusion of artificial and biological membrane vesicles. Fusion of membrane vesicles (in single cells) was observed in terms of their morphology under the microscope, and, at the same time, the quantitative measurement of fusion was carried out for individual vesicles.

In this paper, we present a detailed description of the streak-camera-based time-resolved microscope fluorimeter, its performance, characteristic features, and limitations, and its initial application to the studies of cellular membranes, i.e., peptide-induced membrane fusion in vitro and endosome–endosome fusion in single cells. For the detection of fusion of membrane vesicles, mixing of the lipids or of the contents in the internal aqueous phase of the vesicles was observed by monitoring fluorescence resonance energy transfer. The occurrence of resonance energy transfer decreases the lifetime of the energy donor, which in turn would be detected by time-resolved microscope fluorimetry.

EXPERIMENTAL PROCEDURES

Materials

Bovine serum albumin (BSA),[1] egg-yolk phosphatidylcholine

(PC), and dioleoyl-L-α-phosphatidylcholine (DOPC) were purchased from Sigma (St. Louis, MO), cholesterol (crystallized) and α_2-macroglobulin (α_2M) from Boehringer Mannheim (Indianapolis, IN), [(dichlorotriazinyl)amino]fluorescein (DTAF) from Research Organics (Cleveland, OH), and 5-[2-[(iodoacetyl)amino]ethyl]aminonaphthalene-1-sulfonic acid (IAEDANS), fluorescein-5-maleimide (Fl–mal), 12-(9-anthroyloxy)stearic acid (12-AS), 8-anilinonaphthalene-1-sulfonic acid (ANS), N-(7-nitrobenz-2-oxa-1,3-diazol-4-yl)dipalmitoyl-L-α-phosphatidylethanolamine (NBD-PE), octadecyl rhodamine B chloride (R18), 5-(dimethylamino)naphthalene-1-sulfonyl chloride (dansyl chloride), 4-chloro-7-nitrobenz-2-oxa-1,3-diazol (NBD-Cl), and sulforhodamine 101 (SRh) from Molecular Probes (Eugene, OR).

Methods

Fluorescence Labeling of BSA. BSA (50 mg) was dissolved in 20 mL of 0.1 M NaH_2PO_4/Na_2HPO_4 buffer at pH 7.3, mixed with either IAEDANS or Fl–mal (10 mM in dimethyl sulfoxide) at a final BSA/probe molar ratio of 5:1 (free cysteinyl groups on BSA/probe = 10:1), and incubated at 4 °C for 48 h. Unbound fluorescence probes were removed by extensive dialysis against 0.02 M sodium borate buffer at pH 8.5 for three days with seven changes of 5 L of the dialysis buffer and then against 0.01 M piperazine-N,N'-bis(ethanesulfonic acid) (PIPES) at pH 7.5 for one day with two changes of 5 L of dialysis buffer. By measuring the fluorescence spectrum and the volume of the mixture before and after dialysis, it was found that more than 95% of the labels were consistently bound to BSA under the reaction conditions employed in this work. Therefore, in the following presentation, we assume that probe/BSA ratio is 0.2 and that each BSA molecule contains either 0 or 1 probe molecule. The latter assumption was supported by the time-resolved fluorescence measurement in which we did not detect any indication of resonance energy transfer (self quenching). The probe–BSA conjugates were concentrated with Centriflo (Amicon, Beverly, MA) and mixed with glycerol at a final glycerol concentration of 67% (v/v). The solvent for all the experiments involving BSA reported here was a mixture of glycerol and 0.01 M PIPES buffer (67:33 v/v). Glycerol was added for the ease of sample handling under the fluorescence microscope and for the long-term stability of the protein structure. The probe–BSA solution in the presence of 67% glycerol can be stored at –20 °C in the liquid state for several months without any changes in the fluorescence spectrum and the fluorescence lifetime decay. For observation and measurement under the time-resolved microscope fluorimeter, the probe–BSA conjugates in the aqueous glycerol solution were sandwiched between a cover slip and a slide glass with two spacers (Scotch 810 tape) and sealed with paraffin (Merck, Rahway, NJ).

Preparation of Multilamellar Liposomes with Fluorescent Lipophilic Probes. A multilamellar dispersion of lipids was

---

made by the method of Kusumi et al. (1986). Briefly, a mixture of lipid (egg-yolk PC:cholesterol = 3:2, or DOPC, 1.0 × 10⁻⁶ mol) and the fluorescent probe (12-AS or ANS, 1.0 × 10⁻⁹ mol) in chloroform was dried with a stream of nitrogen gas and further dried under a reduced pressure (~0.1 mmHg) for at least 12 h. The buffer (1 mL) was added to the dried lipid at 37 °C, and the mixture was vortexed vigorously. The buffer used for the study with 12-AS and ANS was 0.1 M sodium borate at pH 9.5. To ensure that all probe carboxyl and sulfonyl groups are ionized in these membranes, a rather high pH was selected (Sanson et al., 1976; Egret-Charlier et al., 1978; Kusumi et al., 1982). Androstane spin label and cholestane spin label, which do not have any ionizable group, did not show ESR spectral change in PC(–cholesterol) membranes between pH 4.5 and 9.5, indicating that the structure of phosphatidylcholine membranes is not influenced by pH in this range (Kusumi et al., 1982). The phase transition temperature (Träuble & Eibl, 1974) and electrostatic properties (Papahadjopoulos, 1968) of phosphatidylcholine membranes are the same in this pH range.

Fluorescence Labeling of Band 3 in the Human Red Blood Cell Ghost. Band 3 molecules, anion channel membrane proteins in the human red blood cell, were labeled with DTAF essentially as described previously (Schindler et al., 1980; Tsuji & Ohnishi, 1986; Tsuji et al., 1988). Briefly, the red blood cells drawn from one of the authors (A.K., type A, Rh⁺) were washed and incubated with 2 mg/mL of DTAF in 0.1 M sodium borate buffer at pH 9.4 at 0 °C for 30 min. The labeled cells were washed four times with Dulbecco's phosphate-buffered saline to remove the unbound label, hemolyzed with 5 mM NaH_2PO_4/Na_2HPO_4, and washed with the same buffer four times. The labeling characteristics was the same as described previously (Tsuji & Ohnishi, 1986; Tsuji et al., 1988).

Measurement of Peptide-Induced Fusion of Liposomes. Bee venom melittin was purchased from Sigma and purified by a slightly modified method of Quay and Condie (1983). Succinylation was carried out by reacting melittin (2 mg) with succinic anhydride (6 mg) for 2 h at room temperature in 2 mL of 20 mM HaH_2PO_4/Na_2HPO_4 buffer at pH 7.2 followed by purification. All four amino groups were succinylated by the reaction (Murata et al., 1987). Two methods were employed to study fusion of liposomes with succinylated melittin at a low pH: (1) the lipid-mixing method and (2) the internal contents mixing method.

(1) The lipid-mixing method: The liposomes containing both NBD-PE (the donor of the resonance energy transfer) and R18 (acceptor) were prepared in the following way (Düzgüneş, 1990; and personal communication). The lipid (NBD-PE: R18:egg-yolk PC, 2.0:0.5:97.5 mol/mol/mol, total 5.2 μmol) was mixed in benzene, and the solvent was removed with a stream of nitrogen and then under a reduced pressure for at least 12 h. The resulting thin film of lipid mixture was hydrated with 1 mL of 150 mM NaCl buffered with 10 mM PIPES at pH 7.4 (PIPES–NaCl buffer) at room temperature and vortexed vigorously for 5 min. The resulting multilamellar vesicles were extruded through polycarbonate membranes (1.0 μm pore diameter, Nucleopore, Pleasanton, CA) to obtain uni- and oligolamellar vesicles of 1–5 μm diameter. Examination of these vesicles by phase-contrast microscopy and electron microscopy confirmed this size. Smaller vesicles were also observed. The vesicles without the fluorophores were prepared by the same method.

Fusion of liposomes was assayed under the fluorescence microscope (the time-resolved microscope fluorimeter) by the following method. The vesicles labeled with both NBD-PE and R18 were mixed with nonlabeled vesicles at a ratio of 1:1. The total lipid concentration was adjusted to 1 mM. The vesicle suspension (20 μL) was mixed with succinylated melittin at a ratio of 1 succinylated melittin/60 lipids. The fusion reaction was initiated by lowering the pH to 5.0 by the addition of 0.5 M citrate buffer and the mixture was incubated at 20 °C for 10 min. As described previsouly (Murata et al., 1987), no fusion was observed at pH 7.4 or without the peptide at pH 5.0. The low-pH-induced fusion with succinylated melittin was stopped by neutralizing the vesicle suspension with 1 M NaOH. In control experiments, the citrate buffer was replaced with PIPES–NaCl buffer. A portion of the resulting mixture (10 μL) was removed and placed between a cover slip and a slide glass and sealed with paraffin for the time-resolved fluorescence measurement under the microscope. When fusion of the labeled and the nonlabeled vesicles takes place, NBD-PE and R18 are diluted in the membrane, resulting in a lower extent of energy transfer, which in turn is detected as the slower fluorescence lifetime decay of NBD.

(2) The internal contents mixing method: Dansyl-dextran was prepared by the following method. *N*-(bromoacetyl)-aminoethylamino-dextran was synthesized from dextran T-40 (average MW of 40 000, Sigma) by the method of Tam et al. (1976). More than 40 amine groups/dextran molecule were introduced. Dansyl chloride (350 μg/mL) and *N*-(bromo-acetyl)aminoethylamino dextran (5 mg/mL) in 0.1 M sodium borate at pH 9.5 were incubated at 4 °C for 16 h. Unreacted fluorophore was removed by dialysis against phosphate-buffered saline with four changes of the buffer. Large unilamellar vesicles (0.2–3 μm in diameter) containing 10 μM dansyl-dextran (energy donor) were prepared by the reverse-phase evaporation method as described by Szoka & Papahadjopoulos (1978) with PIPES–NaCl buffer as the aqueous medium. Small vesicles containing 3.4 mM SRh (acceptor) were prepared by sonication. Untrapped fluorescent markers were removed by gel filtration with Sephadex G75 column chromatography. The final lipid concentration was adjusted to 2 mM. Fusion of liposomes was assayed under the fluorescence microscope (the time-resolved microscope fluorimeter) as described above. Fusion of the dansyl-dextran-loaded and the SRh-loaded vesicles induces mixing of dansyl-dextran and SRh in the fused vesicle, causing resonance energy transfer, which in turn is detected as the faster fluorescence lifetime decay of the dansyl group.

Assay of Endosome–Endosome Fusion in Single Cells. α₂M (Boehringer Mannheim, 3.7 mg/mL) was incubated with 20 μg/mL NBD at pH 9.5 at 4 °C for 17 h. The unbound label was removed by dialysis and column chromatography (Sephadex G-50). The molar ratio of bound NBD/α₂M was typically 3.5. The NIH/3T3 cells cultured on a cover slip were incubated with 1 mg/mL of NBD-α₂M at 18 °C for 10 min, washed with Hanks' balanced salt solution (HBSS) at 4 °C four times, and were further incubated in HBSS either with or without 3 mM SRh at 18 °C for 20 or 60 min. After incubation, the cells were washed with HBSS at 4 °C four times and then fixed with HBSS containing 0.2% (w/w) paraformaldehyde at 4 °C for 2 min. The cells were washed again with HBSS, and the cover glass with the labeled cells was placed upside down on a slide glass with spacers (Scotch 810 tape) and sealed in HBSS with paraffin for observation under the fluorescence microscope and measurement of the fluorescence decay curve. Fusion of the NBD-α₂M-loaded and
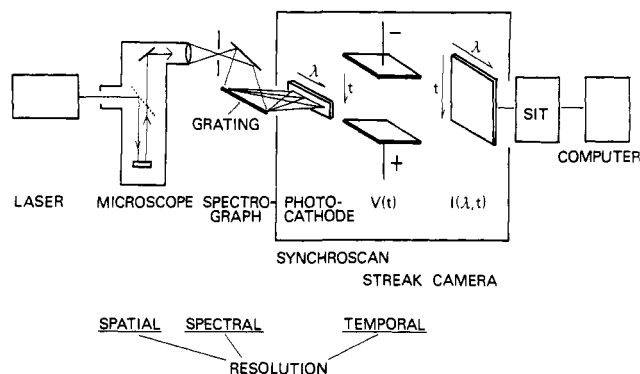
FIGURE 1: Schematic diagram of the time-resolved microscope fluorimeter. The light source is a mode-locked Nd:YAG-based synchronously pumped dye laser (pyridine 1) with cavity dumping. The wavelength is 365 nm, the pulse width is typically 14 ps, the output energy is 3–20 pJ/pulse, and the repetition rate is 4 MHz. The pulsed laser light is guided into the epi-excitation path of the microscope on the optical axis and focused on the sample. The cellular structure of interest is brought to the focused laser spot by mechanically moving the microscope stage. The diameter of the spot used is between 0.8 and 6.3 μm. The fluorescence light emitted from the spot is collected with the objective lens, and then it passes through appropriate barrier filters (or a multichromator) and a pinhole placed at the image plane and finally hits the photoelectric cathode of the synchroscan streak camera. Time resolution (20.2 ps/channel), light detection (with a microchannel plate amplifier), and signal accumulation are accomplished with this streak camera. Details of the streak camera system will be published elsewhere.

SRh-loaded endosomes would induce intermixing of the internal contents in the fused vesicle, causing resonance energy transfer. The Förster distance was estimated to be approximately 5 nm for the dye pair of NBD-α_2M and SRh in solution.

Time-Resolved Fluorescence Measurement under the Fluorescence Microscope. The schematic diagram of the time-resolved microscope fluorimeter we have developed is shown in Figure 1. The instrument consists of five major components: (1) a pulsed light source, a synchronously pumped, cavity-dumped dye laser (pumping by a mode-locked Nd:YAG laser) with second harmonic generation, (2) a fluorescence microscope with epi-illumination and a pinhole unit accessory for selection of a limited area in the microscope view field, (3) a multichromator or a filter unit to select a limited spectral region, (4) a synchroscan streak camera that provides capabilities of time resolution, signal amplification (with a microchannel plate), and signal accumulation, and (5) an image analyzer and a computer to analyze the fluorescence decay curve. Thus, the time-resolved microscope fluorimeter has capabilities of temporal, spatial, and spectral resolution. Details of each component are the following.

(1) The pulsed light source used (Spectra Physics, Mountain View, CA) gives a 4-MHz pulse train of 365-nm excitation light [3–20 pJ/pulse, pulse durations (FWHH) shorter than 14 ps]. A model 3480 continuous wave Nd:YAG laser was mode-locked with a mode locker (models 342A–01 and 453). After frequency doubling (model 3230), the output pulses (a 80.6-MHz pulse train of 532-nm light with pulse durations of ~200 ns at an average power of 800 mW) were used to excite a dye laser (375B-91) with an extended cavity for synchronous pumping and cavity dumping (341-02 and 344-01S). The dye used was 1-ethyl-2-[4-[p-(dimethylamino)-phenyl]-1,3-butadienyl]pyridinium perchlorate (pyridine 1, Lambda Physik, Göttingen, FRG) and a 4.0-MHz pulse train of 730-nm light with pulse durations of ~14 ps at an average power of 50–90 mW was obtained. Finally, after another second harmonic generation (390-01), the 365-nm light pulses

at an average power of 10–50 μW were obtained.

(2) A Zeiss UMSP fluorescence microscope (Oberkochen, FRG) with the UV epi-excitation optics was used. The excitation light from the laser system is guided onto the optical axis of the microscope. All measurements were performed on the optical axis, and the subcellular structure of interest in the microscope view field was brought to the optical axis by moving the microscope stage. The laser beam was focused to form a small circular spot on the sample (0.8–6.3 μm in diameter) with a biconvex lens ($f_0 = 40$ cm) placed in the light steering path and a pinhole placed at the field stop. The fluorescence light emitted from the chosen area was passed through a pinhole placed at the image plane.

(3) Spectral resolution was given with the dichroic mirror system of the microscope and with an Instrument S.A.-Jobin-Yvon HR-320 spectrograph (Longjumeau, France), interference filters (Nihon Shinku, Tokyo, Japan), or long-pass filters (Fuji Film, Tokyo, Japan). For most of the experiments reported in this paper, the filters were used.

(4) The fluorescence light from the microscope was projected onto the slit plane of the synchroscan streak camera (Hamamatsu Photonics K. K., Hamamatsu, Japan. Model C1587 with a modified synchroscan unit of M1955 and a modified plug-in sweep unit of M1954). In this setup, the microscope image can be obtained on the output monitor of the streak camera when the microscope field is homogeneously illuminated, the pinhole on the microscope and the slit on the streak camera were completely open, and the streak camera was used without the time streak (focus mode). The synchroscan unit was modified to allow repetitive scanning at 4 MHz in synchrony with the laser excitation. A synchronization signal from the laser could be obtained by either of the following three methods. (A) A portion of the laser light was detected with a PIN diode (Hamamatsu, C1808) and the output signal was used to trigger the synchroscan streak camera. (B) The mode-locking signal was divided to give a 4-MHz trigger signal. (C) The cavity dumper driver signal was used for triggering. In principle, the method A should give the minimal jitter and would be the best choice. However, we did not observe any difference by employing any of these methods. This is probably due to the fact that the time region we are dealing with is the nanosecond range (the fluorescence lifetime decay) while the system jitter is in the picosecond range. In addition, we adjusted the laser system for good time resolution and long-term stability rather than for maximal average output power. Therefore, for the ease of operation, we employed the cavity dumper signal to trigger the streak sweep (method C above) for most experiments reported here.

The limiting time resolution of the instrument appears to be determined by a complex interplay of the following factors: (A) the light diffraction caused by the focusing lens of the streak camera, (B) the spread of the photoelectrons just after emission from the photocathode, (C) the size of the pinhole placed in the microscope emission path, and (D) the sweep rate. The sweep rate is variable between 20.15 and 80.6 ps/streak channel (487 channels for the full sweep). A–C above induce the spread of the streak image, which is about six streak channels [full width at half-height (FWHH)] for the spot size smaller than 1.6 μm on the sample with a 100× Neofluar objective lens. Therefore, the best time resolution of the instrument without deconvolution with the system response function was estimated to be ~0.12 ns.

Deconvolution of the fluorescence decay curve with the excitation light profile should improve the time resolution. The fluorescence decay curves of Fl-mal and rhodamine B in

ethanol placed between a cover slip and the slide glass was obtained and analyzed with a deconvolution program (Yamashita et al., 1984; Kobayashi et al., 1984). Deconvolution was carried out with the measured excitation light profiles, a delta function, and a gauss function (FWHH = 6–13 channels) mathematically generated in the computer. The results were the same irrespective of the deconvolution function probably because the lifetimes we are interested in (1–20 ns) are much longer than the system response function.

(5) The streak image was read out with a Hamamatsu SIT camera (C1000-18), and the streak image was processed to obtain the fluorescence lifetime decay signal with Hamamatsu C2280 temporal analyzer. The decay curve was analyzed by using an iterative nonlinear least-squares analysis with iterative convolution routines (McKinnon et al., 1977; Yamashita et al., 1984; Kobayashi et al., 1984) on an NEC PC9801 VM2 computer with an Intel 80270 numerical operation coprocessor.

A commercial version of this instrument (Picosecond Fluorescence Microscope System) is now available from Hamamatsu Photonics K. K. (Hamamatsu, Japan. See the tentative specification sheet, No. ETV-188).

The Macroscopic (Cuvette) Configuration for the Time-Resolved Fluorescence Measurement with the Streak Camera. For the measurement in the macroscopic sample configuration (cuvette), the microscope was replaced with a home-built sample chamber with two quartz windows. The excitation laser beam was focused at the center of the cuvette (5 × 5 mm), and the emitted fluorescence was focused on either the inlet slit of the multichromator or the photocathode of the streak camera.

Macroscopic Measurements Using a Method of Time-Correlated Single Photon Counting (TCSPC). As a control for the measurement of fluorescence lifetime decay using the synchroscan streak-camera-based time-resolved microscope fluorimeter, the same sample was measured in a cuvette by the time-correlated single photon counting method (TCSPC, which uses the time-to-amplitude converter). This technique would allow more accurate measurement of the fluorescence decay than analogue methods, such as those using a streak camera.

We have used a standard commercial instrument for this measurement in a cuvette (5 × 5 mm, Photochemical Research Associate Lifetime Instrument type 3000, London, Ontario, Canada). Briefly, TCSPC was carried out with a nanosecond actinic flash lamp (510C) filled with low-pressure hydrogen (≈0.5 atm) operated at a 30-kHz repetition rate (Merkle et al., 1987). The fluorescence decay curves were analyzed for multiple exponentials with deconvolution of the time-dependent lamp intensity profile by using a program FLIMEN from Photochemical Research Associates on a PDP 11-23 computer.

RESULTS AND DISCUSSION

Improvement of the Signal-to-Noise Ratio by Fast Signal Accumulation with a Synchroscan Streak Camera. Figure 2 shows the fluorescence decay curves of 1.4 μM IAEDANS attached to BSA (7 μM) after signal accumulation for (b) 5 and (a) 60 s (20 and 240 million additions of the decay curves, respectively). The decays could be fit to a sum of two exponentials with the time constants of 16.8 and 2.9 ns (92 and 8% of the total fluorescence intensity, respectively). A 40× Neofluar dry objective (numerical aperture = 0.75) was used. The size of the measured spot was 2 μm in diameter, and the measured volume was less than 0.12 pL, containing 1.0 × 10⁵ molecules of IAEDANS–BSA.

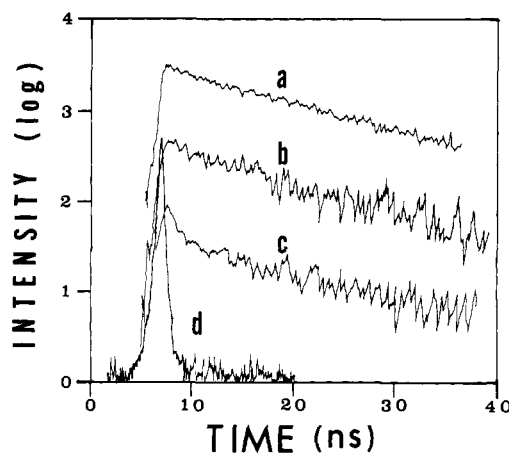As discussed in the previous section, the most difficult technical problem in time-resolved fluorescence measurements

FIGURE 2: Fluorescence decay curves of 1.4 μM IAEDANS attached to BSA (7 μM) after signal accumulation for (b) 5 and (a) 60 s (2.0 × 10⁷ and 2.4 × 10⁸ additions of the decay curves, respectively). A 40× dry objective (numerical aperture = 0.75) was used. The size of the measured spot was 2 μm in diameter, and the measured volume was less than 0.12 pL, containing 1.0 × 10⁵ molecules of IAEDANS–BSA. The decay constants are 16.8 and 2.9 ns (92 and 8% of the total fluorescence intensity, respectively). The fluorescence emission above 410 nm was collected. The decay curves in this figure are vertically shifted for the ease of comparison. (c) The fluorescence decay curve, which shows the presence of rapidly decaying background signal. Conditions: 0.07 μM IAEDANS–BSA, the diameter of the measured spot = 6.3 μm with a 40× Neofluar objective, 1.2 × 10⁸ additions during 30 s. (d) The laser profile (convoluted with the system response function) obtained with a mirror on the sample stage and without the barrier filter in the emission path. Other conditions are the same as in curve a except that the signal was accumulated for 20 s.

under the microscope is to get over the low sensitivity, which is inherent to this type of measurements. The S/N can be improved by signal accumulation, and since we are dealing with labile biological samples, we concentrated our effort on performing the signal accumulation as fast as possible: we accumulated the total fluorescence decays at a rate of 4 MHz (487 points per decay), increasing the S/N of the decay curve by a factor of 2000 during the first second of data acquisition and by a factor of 16 000 during the first minute.

As a check for the systematic noise, the S/N ratio of the decay curve was plotted as a function of the number of signal acquisitions (data not shown). The S/N increases linearly with the square root of the number of additions over 60 s, indicating that the random noise is comparatively larger than the systematic noise that occurs in synchrony with the laser excitation. Due to the limitation of the depth of the frame memory (16 bits) and the thermal dark noise of the SIT camera used for the read-out of the streak image, the continuous data acquisition was limited up to ~70 s. When further signal accumulation was necessary, it was carried out by the addition of separate data files in the computer. This problem could be circumvented by the use of a cooled CCD camera. However, since we are more interested in performing fast measurements on living cells, the duration of signal acquisition was usually kept at less than 60 s.

The approximate guideline for the detection limit of the present instrument is approximately 10⁴ IAEDANS molecules in an area of 2 μm diameter with a 40× Neofluar objective lens, as can be seen from Figure 2. The limit for fluorescein is about the same because the extinction coefficient of fluorescein at 365 nm is low (see Figures 3 and 6 for fluorescein data). The limiting factor for the detectability at the present time is not the sensitivity of the system per se, but the background signal that arises in synchrony with the laser excitation:

Table I: Fluorescence Lifetimes (in ns) of 1 μM IAEDANS–BSA and Fl-mal–BSA in 67% (v/v) Aqueous Glycerol Obtained in the Micro Configuration (Microscope) with the Synchroscan Streak Camera and in the Macro Configuration (Cuvette) by Using either the Streak Camera or the TCSPC Method[a]

| | synchroscan streak camera | | TCSPC |
| | microscope | cuvette | cuvette |
sample			
IAEDANS–BSA	16.8 ± 1.4	16.4 ± 0.4	16.2 ± 0.2
minor component	2.9 (8%)	2.5 (7%)	2.9 (8%)
Fl-mal–BSA	3.15 ± 0.20	3.31 ± 0.15	3.35 ± 0.11
minor component	14–26 (2–5%)	14–20 (2–5%)	9–12 (3–6%)

[a] All decays could be analyzed as a sum of two exponentials.

the leak of the excitation light pulse, and the background fluorescence from the cover and the slide glasses (even quartz), the objective lens, filters, and cells. The background signal has the shorter lifetimes and appears as a sharp peak just after the laser excitation as is partially seen in Figure 2c. The sensitivity limit thereby depends on many factors and cannot easily be generalized. Since the signal intensity from the background increases with an increase of the measured area (Figure 2c), the detection limit in number of fluorophores would be lowered if the fluorophore is locally concentrated in a small volume.

Since the lifetime of these background signal is in the range of subnanosecond to several nanoseconds, fluorophores with longer lifetimes may be measured at lower concentrations by taking advantage of the time resolution. The limitation would also be improved by using an excitation at longer wavelengths and fluorophores that can be excited at longer wavelengths. In the present system, we selected 365 nm as the excitation wavelength so that we could measure a variety of fluorophores without changing the setting of the instrument. At 365 nm, one could excite most of the popular commercial fluorescence probes, such as ANS, dimethylaminonaphthalene (dansyl), anthroyloxyl, diphenylhexatriene, pyrene, NBD, fluorescein, and rhodamine.

The Fidelity of the Decay Rate and the Time Resolution of Two Species of Fluorophores. The decay constants for IAEDANS–BSA and Fl-mal–BSA obtained in the micro configuration (microscope) with the synchroscan streak camera and in the macro configuration (cuvette) with either the streak camera or the time-correlated single photon counting (TCSPC) method are summarized in Table I. It indicates that the measured values agree well when the streak camera method is compared with the TCSPC method in the macro configuration (cuvette). In the micro configuration (microscope), the measured values may be different by ∼5% from those in the cuvette experiments. This may be due to the worse S/N and the higher levels of background fluorescence in the micro configuration.

The time resolution of the instrument is described in detail under Experimental Procedures. We present here the fluorescence decay data for the mixtures of Fl-mal–BSA and IAEDANS–BSA. Such data would help develop a practical "feel" for the time resolution of the instrument. Figure 3 shows the fluorescence lifetime decay obtained for the mixture of IAEDANS–BSA and Fl-mal–BSA at various mixing ratios (2 μM total concentration). Since one of our aims in this work is to make each measurement very quick for the application to biological specimens, we used a signal accumulation time of 17 s for the micro configuration. These results were compared with those obtained with a high accuracy in the macro configuration by using the TCSPC method with the signal accumulation for 2700 s (Figure 3B). For IAEDANS and Fl-mal decays with the difference in decay rate by a factor
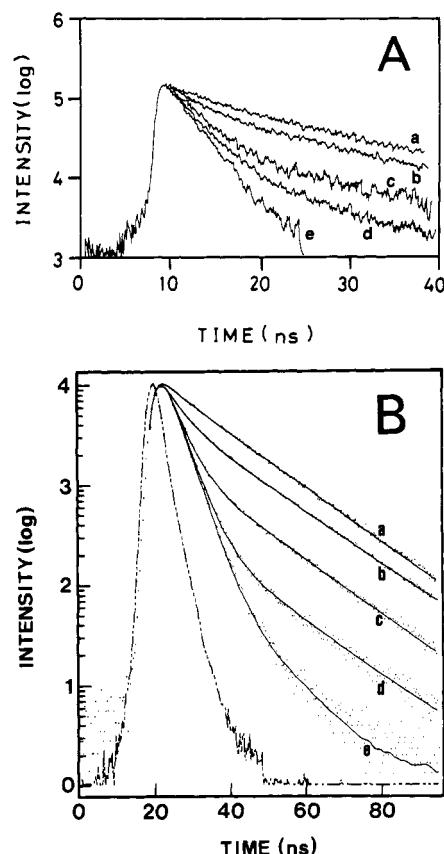

FIGURE 3: Comparison of the data taken with the streak-camera-based time-resolved microscope fluorimeter with those taken by the TCSPC method in the macro configuration. (A) Time-resolved fluorescence measurements under the microscope with a 40× Neofluar objective lens obtained with a synchroscan streak camera. The samples are the mixtures of Fl-mal–BSA and IAEDANS–BSA in 67% (v/v) aqueous glycerol placed between a cover glass and a slide glass with the Scotch tape spacers. The total concentration of IAEDANS–BSA and Fl-mal–BSA is 2 μM. The ratio of IAEDANS and Fl-mal in each sample is (a) 100:0, (b) 90:10, (c) 50:50, (d) 30:70, and (e) 0:100. Conditions: fluorescence emission above 397 nm, the measured area = 6.3 μm in diameter, measured volume ≈ 1 pL, and signal acquisition was for 17 s. (B) Fluorescence lifetime decays obtained in the macro configuration (cuvette) by using the TCSPC method. The excitation wavelength was 355–375 nm (a low-pressure hydrogen spark gap lamp operating at 30 kHz and a Jobin-Yvon monochromator H10), and the fluorescence emission above 450 nm was collected for 2700 s. The total concentration of IAEDANS–BSA and Fl-mal–BSA was 2 μM. The ratio of IAEDANS and Fl-mal in each sample was (a) 100:0, (b) 83:17, (c) 50:50, (d) 17:83, and (e) 0:100.

of about 5, it appears that one could easily detect the presence of 10–30% of the minor species in microscope fluorimetry by a simple examination of the decay curve by eye.

In order to examine further the accuracy of the fluorescence decay constants determined in the micro configuration in the presence of two fluorescence species, various concentrations of IAEDANS–BSA (or Fl-mal–BSA, 1–50 μM) were measured in the presence of 10 μM Fl-mal–BSA (or IAEDANS–BSA). This type of experiment to test the performance of the time-resolved microscope fluorimeter is necessary because the fluorescence decay in cells may be quite complicated due to the variation in the environment in which the fluorophore is located. In addition, we are interested in observing resonance energy transfer to assess the intermolecular distances (The resonance energy transfer decreases the fluorescence lifetime of the energy donor). If the variation of distances exists, the decay would become multiexponential. The result indicates that the lifetimes obtained even at lower concentrations (1–10 μM) are reliable even in the presence
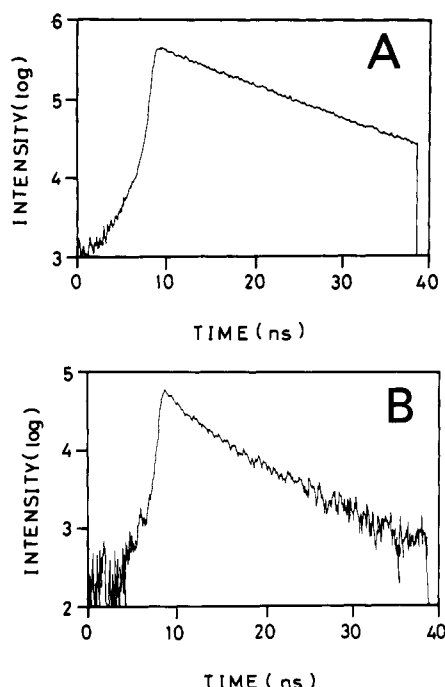
FIGURE 4: Experiments with short signal acquisition time. Signal accumulation was performed for only 2 s. The fluorescence signal (above 410 nm) from an area of 1.6 μm in diameter in a single liposome was measured with a 100× Neofluar objective lens. (A) 12-AS (0.1 mol %) in an egg-yolk PC:cholesterol (2:1) liposome. (B) ANS (0.1 mol %) in a DOPC liposome.

of 10 μM of the other fluorescence species (data not shown). The accuracy depends on the random noise rather than the "pull-in effect" of the other species.

Short-Time Signal Acquisition for Observation of Rapid Processes. Figure 4 shows the decay curves obtained after the signal accumulation for 2 s. The samples are liposomes made of egg-yolk PC and cholesterol (2:1 mol/mol, A) and of DOPC (B) containing 12-AS and ANS at a molar ratio of 1:1000, respectively. The measured area was 1.6 μm in diameter in a single liposome selected under a 100× Neofluar objective lens (numerical aperture = 1.35). The instrument, the laser system and its alignment with the microscope in particular, was carefully optimized for these measurements. The analysis of the decay curves showed that the decay constants are 2.7 and 11.5 ns for 12-AS (A) and 2.3 and 6.9 ns for ANS (B), in complete agreement with the values obtained in the cuvette structure with the TCSPC method [data not shown; for ANS data, see Merkle et al. (1987)]. These results suggest that the instrument described here would be applicable to the study of quite fast cellular processes in single cells. In addition, the S/N ratio in these decay curves suggests that, for the signal acquisition time of 60 s, the fluorescence lifetimes can be determined for $\approx 10^3$ molecules of 12-AS and ANS present in a region of 1.6-μm diameter with a 100× objective.

Application to Single Red Blood Cell Ghost. As the first application to biological membranes, the human red blood cell ghost labeled with DTAF at the anion channel band 3 was used. A S/N ratio better than 30 was obtained for the fluorescence lifetime decay of the labeled ghost measured in a region of 1.6 μm in diameter, containing (2.5–5) × 10^4 molecules of band 3 (because 1.2 × 10^6 copies of band 3 are present in a single erythrocyte and the diameter of the erythrocyte disk is 8 μm) after accumulation of the signal for 30 s (data not shown). The decay time constants are 1.73 and 4.31 ns when the decay curves are analyzed for the double-exponential decay.

One of the most serious problems in fluorescence microscopy is the bleaching of the fluorescence probes due to the photochemical reactions induced by the excitation light. In order to examine the extent of bleaching during the time-resolved measurement, we have carried out the following experiments. A single DTAF-labeled ghost was brought into the focused region of the excitation light of 10 μm in diameter (without changing the excitation light flux). In this way, the ghost was totally inside the measured area, and the effect of lateral diffusion of band 3 going out of and into the focused spot during the measurement was eliminated (Tsuji & Ohnishi, 1986; Tsuji et al., 1988). The fluorescence decay curves were measured intermittently in a region of 6.3 μm in diameter in a single ghost, and the total fluorescence intensity was obtained by integration of the decay curve. No antioxidant was used (in any experiments reported in this paper). The result shows that photobleaching takes place in the first-order kinetics with a time constant of 1460 s under our experimental conditions (data not shown). Since we design all our experiments so that the measurement time is less than 1 min, the maximal photobleaching would be less than 4%. Since fluorescein molecules (and xanthine dyes in general) are notorious for their vulnerability to photo-oxidation, the extent of bleaching would be lower if other flurophores such as rhodamine were used. This low level of bleaching is probably due to the low average excitation power we use (less than 50 W/cm² at the sample) and the short pulse width (14 ps).

Application to the Studies of Peptide–Induced Liposome Fusion. Murata et al. (1987) showed that egg-yolk PC liposomes can be fused by the addition of succinylated melittin and the subsequent incubation at pH 5.0. Neither succinylated melittin alone nor the acid treatment alone induced the fusion of PC liposomes. In the present work, this fusion event was monitored by the time-resolved microscope fluorimetry. Two protocols were used to monitor the liposome fusion: (1) the lipid-mixing method and (2) the internal contents mixing method. The experimental schemes are shown in Figures 5A and 6A, respectively.

(1) The Lipid-Mixing Method. The labeled vesicles containing both NBD-PE (energy donor of the resonance energy transfer) and R18 (acceptor) is mixed with the nonlabeled vesicles. When the fusion of labeled vesicles with nonlabeled vesicles takes place, the extent of resonance energy transfer would be decreased due to dilution of the fluorophores in the membrane, which in turn would be detected as a decrease of the fluorescence decay rate of NBD (Figure 5A). According to Düzgüneş et al. (1987), this method of dilution of donor and acceptor fluorophores is better than observing fusion of vesicles containing only the donors with those containing only the acceptors. In the latter method, resonance energy transfer was observed even when the vesicles are simply aggregated without fusion.

Figure 5B shows the fluorescence lifetime decays of NBD-PE in a region of 1.6-μm diameter in single liposomes. A band-pass filter (427–443 nm) was used to selectively detect the NBD fluorescence by eliminating the fluorescence from R18. With this filter, no R18 fluorescence was detected when the liposomes containing only R18 were examined. The fluorescence lifetime decay is slower after the acid treatment in the presence of succinylated melittin, indicating the decrease of resonance energy transfer and thereby dilution of fluorophores in the membrane, which is induced by vesicle fusion.

Following the acid treatment, considerable variation in decay rate exists among the vesicles, which probably reflects the random process of fusion events in such a mixture. No var-
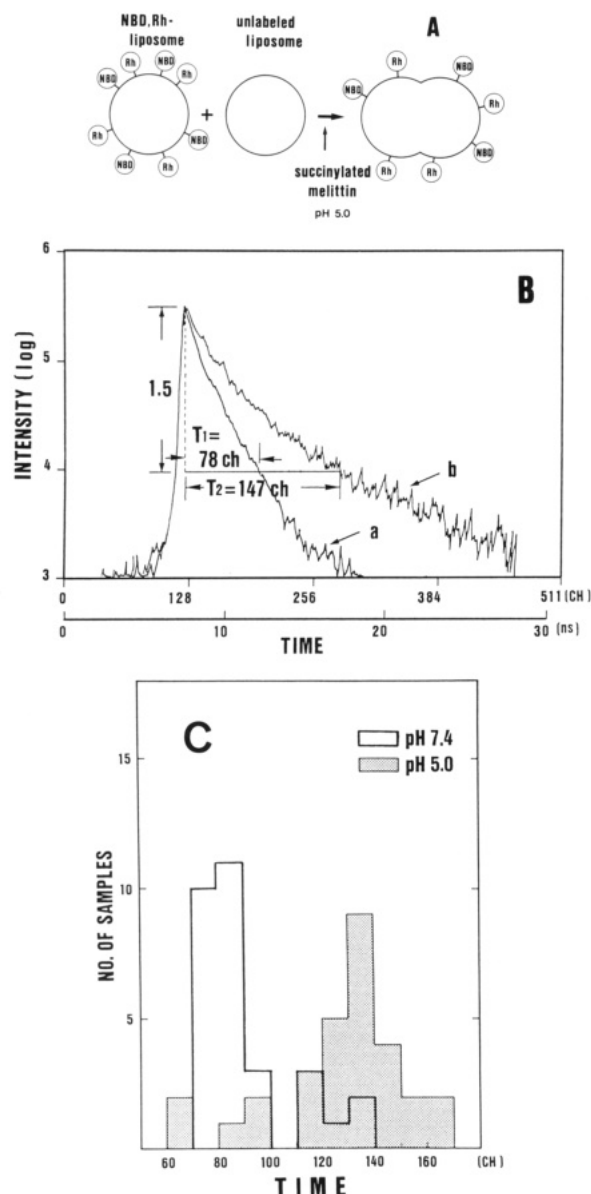
FIGURE 5: (A) Experimental scheme of the lipid-mixing method for the detection of succinylated-melittin-induced liposome fusion at a low pH. The liposomes labeled with both NBD-PE (energy donor) and R18 (acceptor) are mixed with the nonlabeled liposomes. Succinylated melittin is added, and then the mixture was incubated at pH 7.4 or 5.0. The fluorescence lifetime decay curves of NBD-PE in individual vesicles are measured (measured area = 1.6 μm in diameter). Rh represents the rhodamine B group in R18. (B) Typical fluorescence decay curves (a) without and (b) with the acid treatment. Fluorescence emission between 427 and 443 nm (at half transmission). As a convenient measure of the decay rate, the time duration (T, expressed in the streak time channels, 60.3 ps/channel) required for the fluorescence intensity to decrease from its peak value (I) down to $I \times 10^{-1.5}$ (0.0316 $\times$ I) is employed. In the case shown in this figure, T_1 = 78 channels = 4.7 ns (a) and T_2 = 147 channels = 8.9 ns (b). (C) Histogram showing the number of measurements (vesicles) registered at the time duration T. Thirty (30) and 20 vesicles were measured with (hatched) and without (thick line) the acid treatment, respectively. For details, see the text.

iation in NBD lifetime was detected within a liposome. In order to estimate the vesicle-to-vesicle variation, a histogram was made that displays the number of measurements (vesicles) registered for a certain decay time range (expressed in streak time channels, 60.3 ps/channel, Figure 5C). As a convenient measure of the decay rate, the time duration required for the fluorescence intensity to decrease from its peak value (I) down to $I \times 10^{-1.5}$ (0.0316 $\times$ I) was employed (see Figure 5B). This
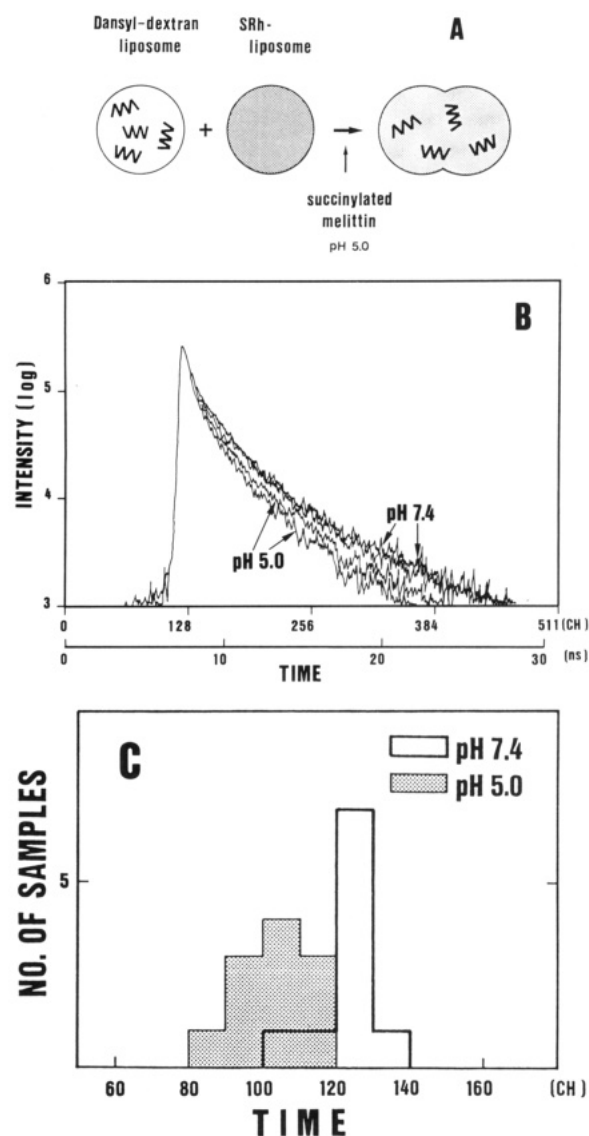
FIGURE 6: (A) Experimental scheme of the internal contents mixing method for the detection of succinylated-melittin-induced liposome fusion at a low pH. The large unilamellar liposomes loaded with dansyl-dextran (donor) were mixed with the small vesicles loaded with SRh (acceptor). After the incubation with succinylated melittin at pH 7.4 or 5.0, the fluorescence lifetime decay curves of dansyl-dextran in individual vesicles were measured (measured area = 1.6 μm in diameter). (B) Typical fluorescence decay curves of dansyl-dextran (a) without and (b) with the acid treatment. Fluorescence emission between 427 and 443 nm. (C) Histogram showing the number of vesicles registered at the time duration T. A total of 11 measurements (of vesicles) were carried out with (hatched) and without (thick line) the acid treatment. For details, see text.

type of simplistic analysis was necessary because the fluorescence decay was very complex. The decay curve could not be fit to a sum of three exponentials.

The histogram shown in Figure 5C summarizes the results of the measurements for 30 vesicles after the acid treatment and for 20 vesicles without the acid treatment. (Before fusion, larger liposomes with a diameter between 2 and 5 μm were selectively measured. The shape of the histogram is similar to that produced on the basis of the measurements of an area that contains several smaller liposomes.) In spite of the variation from one vesicle to another, the difference between the samples with and without the acid treatment is clear. The variation in the decay rate is larger in the sample treated with the low pH, reflecting the random fusion events, in which some labeled vesicles fused with nonlabeled vesicles more than

others. This result suggests that, for the analysis of complex fusion processes, such measurements on individual vesicles are important. Further analysis of fusion processes is in progress in our laboratories.

(2) *The Internal Contents Mixing Method (Figure 6).* Large unilamellar vesicles formed by the reverse-phase evaporation method (Szoka & Papahadjopoulos, 1978; 0.1–3 μm in diameter) that contain dansyl-dextran in their internal aqueous volume are incubated with small vesicles that contain water-soluble SRh ($\approx$0.03–0.07 μm in diameter). The fusion of these vesicles would induce the mixing of the internal aqueous compartments, which would result in the occurrence of resonance energy transfer from dansyl to SRh (Figure 6A). The concentration of dansyl-dextran in the liposome was 10 μM. The measurement of the decay rate of dansyl-dextran in solution showed that further dilution of dansyl-dextran does not change the decay rate, warranting that dilution of dansyl-dextran after fusion and possible leakage of dansyl-dextran at the time of fusion would not affect the measurement of the fluorescence lifetime decay. This is one of the important advantages of using the lifetime decay as the experimental observable, as compared to the fluorescence intensity measurement at the steady state, in which both resonance energy transfer and dilution can cause decreases of the fluorescence intensity of the donor.

Figure 6B shows the fluorescence lifetime decays of dansyl-dextran observed in individual vesicles with a measuring spot diameter of 1.6 μm on the sample. The fluorescence lifetime decay is faster after the acid treatment in the presence of succinylated melittin, indicating the occurrence of resonance energy transfer and thereby mixing of the internal contents.

A histogram such as that shown in Figure 5C was made that displays the number of measurements ($\approx$ vesicles, because no variation in a vesicle was detected) registered for a certain decay time range (Figure 6C). In spite of the variation from one vesicle to another, the difference between the samples with and without the acid treatment is clear. The variation in the decay rate is larger in the sample treated with the low pH, in agreement with the data obtained with the lipid-mixing method.

Application to the Study of Endosome–Endosome Fusion in Single Cells. Time-resolved microscope fluorimetry was applied to the quantitative assay of endosome–endosome fusion in cultured single cells. This technique allows quantitative measurements on individual endosomes, while the endosomes and the cells are being viewed under a high magnification objective lens. As a quantitative measure of the endosome fusion, intermixing of the internal contents of endosomes was monitored by detecting resonance energy transfer: when endosomes containing the energy donor and those containing the energy acceptor fuse, resonance energy transfer would be induced due to the mixing of the donor and the acceptor in the fused endosomes, which would result in acceleration of the fluorescence decay of the energy donor. This is a direct application of the liposome fusion assay by the internal contents mixing method described above.

The experimental scheme is shown in Figure 7A. First, the NIH/3T3 cells were incubated with NBD-α_2-macroglobulin (α_2M, energy donor) at 18 °C for 10 min, and after washing at 0 °C, the cells were further incubated with water-soluble SRh (energy acceptor) at 18 °C for various durations. This method, thereby, produces endosomes containing the donor and those loaded with the acceptor in sequence. Thus, we try to develop a convenient method to observe fusion of sequentially formed endosomes in single cells.

Since later fusion events, such as fusion of endosomes with primary lysosomes, are known to be inhibited below 20 °C, the experiments were carried out at 18 °C to observe only endosome–endosome fusion (Dunn et al., 1980).

Figure 7B shows one of the cells incubated as described. The numerous fluorescent spots show the endosomes loaded with the fluorescent molecules. Elongated tubulovesicular bodies (3–10 μm) that were loaded with SRh were sometimes observed. The excited-state lifetime of NBD was measured mostly for individual endosomes (The cells were fixed with 0.2% paraformaldehyde just before the microfluorimetric measurements for the ease of sample handling). The curves shown in Figure 7C are typical fluorescence decays of NBD-α_2M (donor) in individual endosomes in cells that were subsequently incubated with and without the energy acceptor. Because the fluorescence decay is faster in the cells incubated with the acceptor, this result indicates the occurrence of resonance energy transfer in endosomes, which, in turn, suggests that the fusion of sequentially formed endosomes takes place in cells and that it can be detected by this technique. The endosome fusion occurs more extensively with incubation for 60 min than for 20 min.

Since considerable variation in decay rate was observed from one endosome to another, we have measured many endosomes and constructed a histogram as we did in Figures 5C and 6C (Figure 7D). [The measurement was made for mostly single endosomes although, in some cases, several endosomes may be detected that are located either adjacent to each other or at various focal planes. Another histogram (not shown) produced from the measurements in which a few endosomes were always detected through the measuring pinhole is similar to that shown in Figure 7D.] The histogram indicates that extensive fusion of sequentially formed endosomes takes place in cells. Since the method developed here cannot detect the fusion of two donor endosomes or that of two acceptor endosomes, this result suggests that more than half of the endosomes are fused endosomes after a 20-min incubation with SRh.

These results are in general agreement with the following model in which multiple fusion events of sequentially formed endosomes and/or sequential fusion events of endosomes with another endocytic compartment, such as a (hypothetical) sorting organelle (Salzman & Maxfield, 1988), and with the endosomal network of tubular cisternae (Hopkins et al., 1990) take place in many parts of the cell. In addition, our results indicate that (α_2M) receptor-positive endosomes and pinocytic vesicles fuse, which agrees with the data of Salzman and Maxfield (1988) and Ward et al. (1990).

CONCLUSIONS

We have described a newly developed time-resolved microscope fluorimeter that is based on a synchroscan streak camera and laser excitation with a high repetition rate. The improvement of S/N per unit time was enhanced by acquiring the total fluorescence decay (487 points) at a rate of 4 MHz. The fluorescence lifetime decay was obtained for 10^3–10^5 fluorophores in a small spot (0.8–6.3 μm in diameter) under the fluorescence microscope during 2–60 s. With the instrument developed here, time-resolved microscope fluorimetry has, for the first time, become a practical tool for investigation of molecular processes in biological systems while they are viewed under the fluorescence microscope with a high-power objective. This method, thus, initiates the development of a new generation of microfluorimetry for biology and medicine. It has opened up a possibility of fluorescence lifetime imaging, in
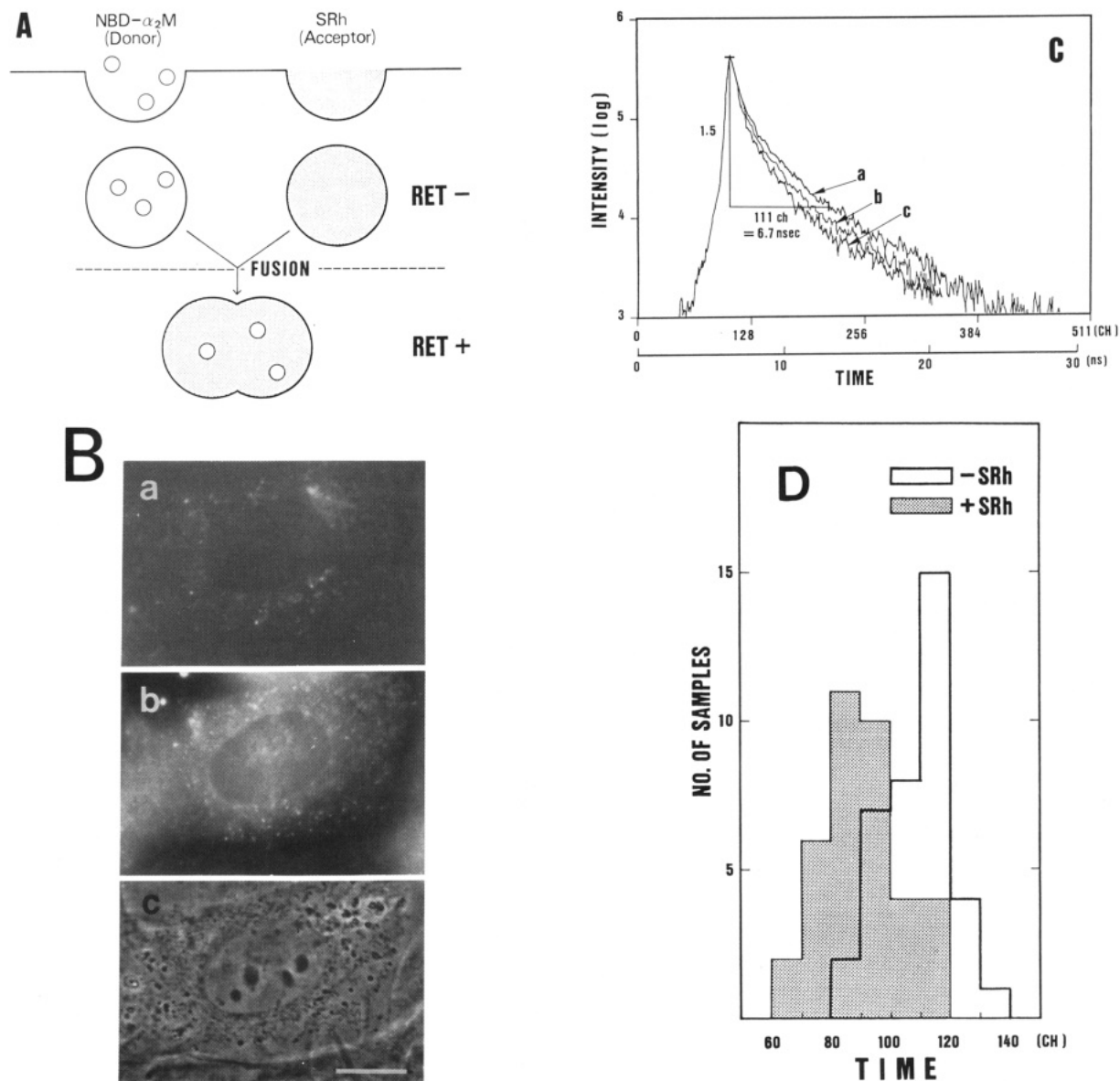
FIGURE 7: (A) Experimental scheme showing the method for the detection of fusion of the sequentially formed endosomes in single cells. RET represents resonance energy transfer. (B) NIH/3T3 cells incubated with NBD-α_2M (energy donor) and then with SRh (acceptor): observation of the same cell in the NBD channel (a, 427–443 nm) and in the rhodamine channel (b, above 590 nm) of the fluorescence microscope and by phase contrast microscopy (c). (C) Fluorescence lifetime decays of NBD measured for individual endosomes: incubation without SRh (a), and incubation with SRh for 20 min (b) and 60 min (c). (D) Histogram showing the number of endosomes registered in the time duration *T*. [Open bars (thick line)] incubation without SRh; (hatched bars) incubation with SRh for 20 min.

which the microscope image contrast is generated on the basis of the fluorescence lifetime.

This technique has been applied to detection of resonance energy transfer to monitor the fusion of membrane vesicles in vitro and in vivo. It has allowed us to examine individual liposomes in vitro and endosomes in single cells. These initial applications illustrate the usefulness of simultaneous acquisition of morphological and molecular information under the fluorescence microscope in understanding dynamic biological processes such as endosome fusion in cells.

Fusion of sequentially formed endosomes in vivo has been shown by the time-resolved microscope fluorimetry. Since the use of time-resolved microscope fluorimetry eliminates the need for complex correction procedures (Salzman & Maxfield, 1988) or subcellular fractionation (Ajioka & Kaplan, 1987; Ward et al., 1990), it greatly simplifies the assay for endosome fusion in vivo.

In the present research, we observed that (1) fusion of endosomes takes place at 18 °C, (2) more than half of the endosomes are fused endosomes after a 20-min incubation with SRh, (3) more extensive mixing of the endosome contents takes place after a 60-min incubation with SRh, and (4) fused endosomes are scattered all over the cell matrix. Previously, Salzman and Maxfield (1988) indicated that the fusion of endocytic compartments containing transferrin–receptor complex and pinocytosed immunoglobulin G takes place either in sorting endosomes or later along the receptor-recycling pathway such as in the para-Golgi. Since para-Golgi is unlikely to be involved in the endocytic pathway of α_2M, our results are consistent with a model in which many numbers of endosomal compartments, possibly sorting organelles, are formed at which extensive fusion with incoming endosomes takes place (Ward et al., 1990; Salzman & Maxfield, 1988). Another possibility we would like to raise is the involvement of an extensive network of tubular cisternae of the endosomal compartment, as reported by Hopkins et al. (1990). The early endosomes would fuse with this compartment at many points in the network. The reason why we did not detect such a

tubulovesicular endosomal network may be that the cells were lightly fixed before observation (Hopkins et al., 1990).

The time-resolved microfluorimetric assay developed in the present work would be useful in investigating fusion events of other endocytic organelles and the traffic of receptors and ligands in cells and in searching for membranous and cytosolic factors that induce membrane fusion in cells. A detailed study of the time course of endosome–endosome and endosome–lysosome fusion is in progress in our laboratories.

In conclusion, time-resolved microscope fluorimetry is a useful new method to study a variety of processes occurring in cells in culture. It is a powerful, noninvasive technique to advance the studies of in situ biochemistry and biophysics using cells and tissues.

ACKNOWLEDGMENTS

REFERENCES

Ajioka, R. S., & Kaplan, J. (1987) *J. Cell Biol. 104*, 77–85.

Alsins, J., Claesson, S., & Elmgren, H. (1982) *Chem. Scr. 20*, 183–187.

Andreoni, A., Longoni, A., Sacci, C. A., & Svelto, O. (1980) in *The Biomedical Laser: Technology and Clinical Applications* (Goldman, L., Ed.) pp 69–83, Springer, New York.

Bottiroli, G., Cionini, P. G., Docchio, F., & Sacchi, C. A. (1984) *Histochem. J. 16*, 223–233.

Docchio, F., Longoni, A., Ramponi, R., Sacchi, C. A., Bottiroli, G., & Freitas, I. (1982) *Proc. SPIE—Int. Soc. Opt. Eng. 369*, 16–21.

Dunn, W. A., Hubbard, A. L., & Aronson, N. N., Jr. (1980) *J. Biol. Chem. 255*, 5971–5978.

Düzgüneş, N. (1990) *Methods Enzymol.* (in press).

Düzgüneş, N., Allen, T. M., Fedor, J., & Papahadjopoulos, D. (1987) *Biochemistry 26*, 8435–8442.

Egret-Charlier, M., Sanson, A., Ptak, M., & Bouloussa, O. (1978) *FEBS Lett. 87*, 313–316.

Fernandez, S. M., & Berlin, R. D. (1976) *Nature 264*, 411–415.

Herman, B. A., & Fernandez, S. M. (1978) *J. Cell Physiol. 94*, 253–264.

Herman, B. A., & Fernandez, S. M. (1979) *Arch. Biochem. Biophys. 196*, 430–435.

Herman, B. A., & Fernandez, S. M. (1982) *Biochemistry 21*, 3275–3283.

Hopkins, C. R., Gibson, A., Shipman, M., & Miller, K. (1990) *Nature 346*, 335–339.

Kobayashi, S., Yamashita, M., Sato, T., & Muramatsu, S. (1984) *IEEE J. Quantum Electron. QE-20*, 1383–1386.

Kusumi, A., Subczynski, W. K., & Hyde, J. S. (1982) *Fed. Proc. 41*, 1394, Abstract 6571.

Kusumi, A., Subczynski, W. K., Pasenkiewicz-Gierula, M., Hyde, J. S., & Merkle, H. (1986) *Biochim. Biophys. Acta 854*, 307–317.

McKinnon, A. E., Szabo, A. G., & Miller, D. R. (1977) *J. Phys. Chem. 81*, 1564–1570.

Merkle, H., Subczynski, W. K., & Kusumi, A. (1987) *Biochim. Biophys. Acta 897*, 238–248.

Minami, T., & Hirayama, S. (1986) *Ionics*, 11–16 (in Japanese).

Minami, T., Kawahigashi, M., Sakai, Y., Shimamoto, K., & Hirayama, S. (1986) *J. Lumin. 35*, 247–253.

Murata, M., Nagayama, K., & Ohnishi, S. (1987) *Biochemistry 26*, 4056–4062.

Papahadjopoulos, D. (1986) *Biochim. Biophys. Acta 163*, 240–254.

Quay, S. C., & Condie, C. C. (1983) *Biochemistry 22*, 695–700.

Sacci, C. A., Svelto, O., & Prenna, G. (1974) *Histochem. J. 6*, 251–258.

Salzman, N. H., & Maxfield, F. R. (1988) *J. Cell Biol. 106*, 1083–1091.

Sanson, A., Ptak, M., Rignaud, J. L., & Gary-Bobo, C. M. (1976) *Chem. Phys. Lipids 17*, 434–444.

Schindler, M., Koppel, D. E., & Sheetz, M. P. (1980) *Proc. Natl. Acad. Sci. U.S.A. 77*, 1457–1461.

Szoka, F., Jr., & Papahadjopoulos, D. (1978) *Proc. Natl. Sci. U.S.A. 75*, 4194–4198.

Tam, S.-C., Blumenstein, J., & Wong, J. T.-F. (1976) *Proc. Natl. Acad. Sci. U.S.A. 73*, 2128–2131.

Taylor, D. L., & Salmon, E. D. (1989) *Methods Cell Biol. 29*, 207–237.

Thaer, A. A., & Sernetz, M. (1973) *Fluorescence Techniques in Cell Biology*, Springer, Berlin.

Träuble, H., & Eibl, H. (1974) *Proc. Natl. Acad. Sci. U.S.A. 71*, 214–219.

Wang, X. F., Kitajima, S., Uchida, T., Coleman, D. M., & Minami, S. (1990) *Appl. Spectrosc. 44*, 25–30.

Ward, D. M., Hackenyos, D. P., & Kaplan, J. (1990) *J. Cell Biol. 110*, 1013–1022.

Yamashita, M., Nomura, M., Kobayashi, S., Sato, T., & Aizawa, K. (1984) *IEEE J. Quantum Electron. QE-20*, 1363–1367.